ELSEVIER

Journal of Nuclear Materials 303 (2002) 83–91

journal of nuclear materials

www.elsevier.com/locate/jnucmat

Temperature effect of dynamic anisotropic elastic constants of Zr–2.5Nb pressure tube by resonant ultrasound spectroscopy

Yong-Moo Cheong *, Sung-Soo Kim, Young-Suk Kim

Pressure Tube Materials Group, Korea Atomic Energy Research Institute, P.O. Box 105, Yusong, Taejon 305-600, South Korea

Received 10 September 2001; accepted 6 April 2002

Abstract

Dynamic anisotropic elastic constants of CANDU Zr–2.5Nb pressure tube materials were determined by high temperature resonant ultrasound spectroscopy (RUS). The resonance frequencies were measured using a couple of alumina waveguides and wide-band ultrasonic transducers in a small furnace. The rectangular parallelepiped specimens were fabricated along with the longitudinal, radial and transverse direction of the pressure tube. The initial estimates for RUS were obtained from the orientation distribution function by X-ray pole figure and elastic stiffness of single crystal zirconium. A nine elastic stiffness tensor for orthotropic symmetry was determined in the range of room temperature ~500 °C. As the temperature increases, the elastic constant tensor, c_{ij} gradually decreases. Higher elastic constants along the transverse direction compared to those along the longitudinal or radial direction are similar to the case of Young's modulus or shear modulus. A crossing of elastic constants along the longitudinal direction and radial direction was observed near 120–150 °C. This fact could correlate to the crossing characteristics of c_{44} and c_{66} of a zirconium single crystal in the temperature range.

PACS: 62.20.D

1. Introduction

The elastic moduli of materials are important in engineering, such as in mechanical design, fracture analysis and life-time estimation. To determine the elastic moduli requires many samples with different compositions, fabrication processes and heat treatments. For anisotropic materials, such as composite materials or textured materials, it is more difficult to determine the elastic moduli.

Resonant ultrasound spectroscopy (RUS) is used to determine the elastic stiffness for various shapes of samples, i.e. spherical, cylindrical, or rectangular parallelepiped. Theoretically, a maximum of 21 tensor elements of elastic stiffness for the triclinic crystal (the lowest-symmetry crystal) can be determined with one specimen. However, for such a low-symmetry crystal, it is difficult to assimilate properties relating to stress waves and elasticity [1]. Practically, RUS can determine nine tensor elements for orthotropic symmetry as well as higher-symmetry, such as isotropic, cubic, hexagonal and tetragonal symmetry.

One of the key elements in RUS is to determine the symmetry and the initial estimate of elastic stiffness in advance. The initial estimate should be close to the true value and can be obtained from the literature, experience, other measurements, etc. The test sample should be machined accurately. The calculated resonance frequencies and modes should be matched to the measured values by RUS and the elastic stiffness can be converged by comparison and iteration.

The Zr–2.5Nb alloy for the pressure tubes in CANDU (CANadian Deuterium Uranium) reactors have developed a strong texture due to the limited slip system during the extrusion process, leading to anisotropic properties. The material properties strongly depend on

* Corresponding author. Fax: +82-42 868 8346.
E-mail address: ymcheong@kaeri.re.kr (Y.-M. Cheong).

0022-3115/02/$ - see front matter
PII: S0022-3115(02)00847-4

the orientation distributions of grains, which result in a directional anisotropy of elastic stiffness, thermal expansion coefficients, etc. To characterize the degree of anisotropy, it is necessary to correctly determine the anisotropic elastic moduli depending on the direction of the tube samples. The anisotropy of the Zr–2.5Nb alloy could be treated as orthotropic symmetry, consisting of three principal coordinates such as radial, transverse and longitudinal direction.

Initial approximated elastic stiffness has been estimated by the orientation distribution function (ODF) from X-ray pole figure data and the elastic stiffness of single crystal zirconium. Based on the initial estimates, anisotropic elastic stiffness of the Zr–2.5Nb alloy has been determined by RUS. Temperature dependency of anisotropic elastic constants of the Zr–2.5Nb materials was determined by high temperature RUS based on the room temperature values of the anisotropic elastic constant. A nine elastic stiffness tensor for the orthotropic symmetry was determined in the range of room temperature ~500 °C.

2. ODF and anisotropic elastic stiffness

Polycrystalline Zr–2.5Nb pressure tube materials is a hexagonal closed packed (hcp) structure and is textured along the circumferential direction. The elastic stiffness on the tubular sample coordinate (longitudinal, radial and circumferential directions) can be expressed as an orthotropic symmetry and represented as

$$c_{ij} = \begin{pmatrix} c_{11} & c_{12} & c_{13} & 0 & 0 & 0 \\ c_{12} & c_{22} & c_{23} & 0 & 0 & 0 \\ c_{13} & c_{23} & c_{33} & 0 & 0 & 0 \\ 0 & 0 & 0 & c_{44} & 0 & 0 \\ 0 & 0 & 0 & 0 & c_{55} & 0 \\ 0 & 0 & 0 & 0 & 0 & c_{66} \end{pmatrix}. \quad (1)$$

Macroscopic properties of a sample, $\overline{E}$ can be obtained by the integration of the properties, $E(g)$ depending upon the orientation of an individual grain, g and weighting factor, i.e. ODF of grains, $f(g)$ along the total orientation space [2]:

$$\overline{E} = \int E(g) \cdot f(g) \mathrm{d}g. \quad (2)$$

In order to represent the elastic stiffness tensor of rank = 4 to 6×6 matrix form, the usual four-to-two contraction scheme is adopted: $11 \to 1$, $22 \to 2$, $33 \to 3$, $23 \to 4$, $13 \to 5$ and $12 \to 6$.

The anisotropy of the polycrystalline with textured structure can be calculated as an average of the material properties of each grain if interactions between grains are negligible. The averaged elastic stiffness along the sample coordinate can be estimated by knowing the elastic stiffness of a single crystal and the orientation distribution of grains from the pole figure data by X-ray or neutron diffraction. Based on the pole figure data, the ODF can be calculated by generalized spherical harmonics and series expansion coefficients [3]:

$$\omega(\xi, \phi, \varphi) = \sum_{l=0}^{4} \sum_{m=l}^{4} \sum_{n=-l}^{4} W_{lmn} Z_{lmn} \mathrm{e}^{-\mathrm{i}m\phi} \mathrm{e}^{-\mathrm{i}n\varphi}, \quad (3)$$

where $\omega(\xi, \phi, \varphi)$ is ODF for the standard Euler angles (ξ, ϕ, φ) between the global coordinate system and local coordinate system, Z_{lmn} is the generalized Legendre polynomial defined by Roe [4], W_{lmn} is the series expansion coefficient adopted from Roe, or notation by Bunge [5]. When a tensor rank with p is averaged, W_{lmn} includes the elements of $l \leqslant p$, which implies a maximum number tensor element, l, m and n is 4 for the case of an elastic stiffness tensor. W_{lmn} and Z_{lmn} for orthotropic symmetry have been calculated by Morris [6].

In order to explain actual elastic stiffness, various models or approximations have been suggested. Based on the orientation distribution by a sample coordinate, the elastic stiffness can be estimated by either Voigt's approximation, the Reuss approximation, or the self-consistent iteration method, etc. Voigt's approximation assumes that the total stress is a sum of the individual stresses on each grain, whereas in the Reuss approximation a sum of the individual strains on each grain is assumed. Both approximations represent two extreme cases and can be regarded as upper and lower bounds [7]:

$$\overline{c_{ijkl}} = \frac{1}{8\pi^2} \int c_{ijkl}(\Omega) \mathrm{d}\Omega \quad \text{(Voigt's approximation)}, \quad (4)$$

$$\overline{S_{ijkl}} = \frac{1}{8\pi^2} \int S_{ijkl}(\Omega) \mathrm{d}\Omega \quad \text{(Reuss approximation)}, \quad (5)$$

where $\overline{c_{ijkl}}$ and c_{ijkl} are the averaged and individual elastic stiffness, $\overline{S_{ijkl}}$ and S_{ijkl} are the averaged and individual elastic compliance, Ω is Euler angles, θ, ϕ, φ and $\int \mathrm{d}\Omega = 8\pi^2$.

3. Elastic stiffness by resonant ultrasound spectroscopy

Free vibration or resonance is sensitive to the microscopic and macroscopic properties of the materials. Because RUS can determine accurate elastic stiffness and ultrasonic attenuation, it can be applied to materials characterization, non-destructive testing, etc. [8]. An exact analytical solution of the free vibration problem to determine resonance frequencies is not known or available a priori. Only approximated solutions are available by numerical analysis, such as the finite element method or minimization of energy. The fundamental theory of resonance was developed by Maynard [9], and theoret-

ical calculations and experiments for the resonance of an elastically isotropic rectangular parallelepiped specimen were made by Holland [10] and Demarest [11]. Those results were generalized by Ohno [12] and comprehensive applications to the solid-state physics were made by Migliori et al. [13].

The eigenvector or eigenfrequency of vibrating solids can be calculated by a theory of the minimization of energy, i.e. a mechanical Lagrangian of elastic solids with some approximations. In classical mechanics, the solution to Lagrangian for free vibration can be expressed as the elastic wave equation,

$$\rho\omega^2 u_i + \sum_{j,k,l} c_{ijkl} \frac{\partial^2 u_k}{\partial x_j \partial x_l} = 0. \tag{6}$$

This equation is solved subject to the vanishing of the ith component of the surface traction vector,

$$\sum_{j,k,l} \vec{n_j} c_{ijkl} = \sum_{j} \vec{n_j} \sigma_{ij} = 0, \tag{7}$$

where ρ is density, ω is frequency, u_i is the ith component of the displacement vector, c_{ijkl} is the elastic modulus tensor, n_j is the unit vector normal to the surface and σ_{ij} is the stress tensor. While the direct (forward) problem (calculation of resonance frequencies based on sample description) is challenging in its own right, the inverse problem (calculation of elastic constants from measured frequencies) is considerably more difficult. A combination of u_i satisfying those conditions is displacement corresponding to the normal mode free vibration frequency. Based on this fact, an algorithm for the calculation of frequencies corresponding to the minimization of energy using the Rayleigh–Ritz method was developed by Demarest [11]. The resonance frequencies can be calculated for a sample with known density, dimension, orientation and elastic stiffness. Actually, because the solution of the inverse problem is not simple and no exact solution is available, non-linear optimization procedures are the best option. A computer code has been developed based on a fast and efficient solution of the direct problem, which is then used in an iterative Levenburg–Marquardt scheme to solve the inverse problem with the figure of merit [14].

4. Experimental

4.1. Specimen

Nuclear grade Zr–2.5Nb CANDU pressure tube materials are used as specimens. From the pole figures of (0002), $(10\bar{1}0)$ and $(10\bar{1}1)$ for the Zr–2.5Nb alloy shown in Fig. 1, this material exhibits a strong textured structure due to extrusion processes.

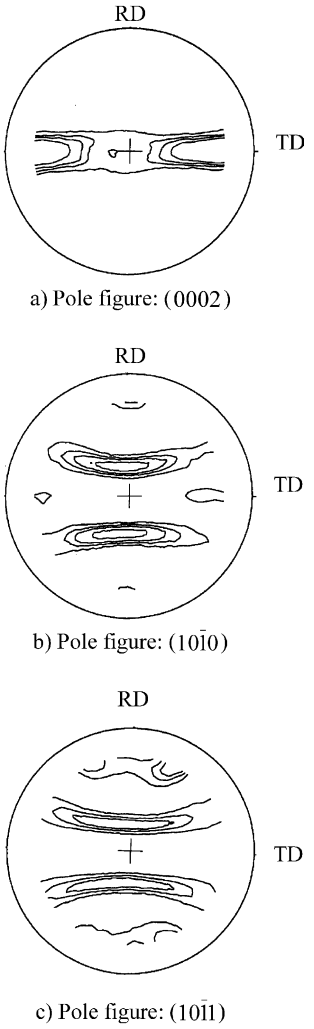

Fig. 1. Pole figures for Zr–2.5Nb pressure tube materials.

4.2. Calculation of the initial estimate of anisotropic elastic stiffness

The ODF of the Zr–2.5Nb alloy has been calculated using a computer program, 'popLA', by the Los Alamos National Laboratory [15]. The raw data file of the X-ray pole figure was converted to the ASCII format as required by the program. The angles of orientation distribution can be represented by one of the notations by Euler, Roe-Matties or Bunge [15].

With the elastic stiffness of single crystal zirconium [16], shown in Table 1, and the weight factor of individual grains obtained from the ODF, the averaged elastic stiffness of the polycrystalline Zr–2.5Nb alloy has been obtained using Voigt's approximation, the Reuss approximation, or the self-consistent method by iteration. The subscripts in Table 1 are referred to as the

Table 1
Elastic stiffness of single crystal zirconium (hcp) [16] (unit: 10^{11} N/m^2)

$c_{11} = c_{22}$	c_{33}	c_{44}	$c_{66} = \frac{1}{2}(c_{11} - c_{12})$	c_{13}	c_{12}
1.434	1.648	0.320	0.353	0.653	0.728

Notation of hcp single crystal: $1(=2) = a$-axis, $3 = c$-axis.

Table 2
Anisotropic elastic stiffness of Zr–2.5 Nb pressure tube materials by ODF model (unit: 10^{11} N/m^2)

	c_{11}	c_{22}	c_{33}	c_{23}	c_{13}	c_{12}	c_{44}	c_{55}	c_{66}
Voigt's approximation	1.449	1.490	1.446	0.687	0.699	0.713	0.340	0.343	0.375
Reuss approximation	1.437	1.473	1.440	0.691	0.702	0.720	0.338	0.341	0.365
Self-consistent	1.443	1.482	1.443	0.689	0.700	0.717	0.339	0.342	0.370

Notation of sample orientation: 1 = RD (radial direction), 2 = TD (transverse direction), 3 = LD (longitudinal direction).

crystallite coordinate, i.e. $1(=2) = a$-axis, $3 = c$-axis in the hcp single crystal orientation.

Initial estimates of the elastic stiffness of the polycrystalline Zr–2.5Nb alloy are shown in Table 2. The subscripts refer the tubular sample coordinate, i.e. 1 = radial, 2 = transverse and 3 = longitudinal direction. The anisotropic nature along longitudinal, radial and circumferential directions can make it the orthotropic symmetry, which requires a nine independent elastic stiffness.

4.3. Determination of anisotropic elastic stiffness by RUS

The high temperature RUS device was assembled as shown in Fig. 2. A small furnace and a temperature controller were attached to the basic RUS device, which consists of a synthesizer to generate continuous frequencies and two wide-band ultrasonic transducers for sending and receiving signals in a vacuum system. In order to measure the resonance frequency at the high temperature, the specimen was inserted between two wave guides with ultrasonic transducers, one is a transmitter and the other is a receiver. Minimal force was applied in order to hold the specimen at the corners to allow free vibration of the specimen, and controlled accurately (<1 g) by a load cell, spring device, and positioning device. The thermocouple should not be in contact to the specimen because the resonance frequencies and modes are influenced by the contact. In order to control the specimen temperature in the vac-

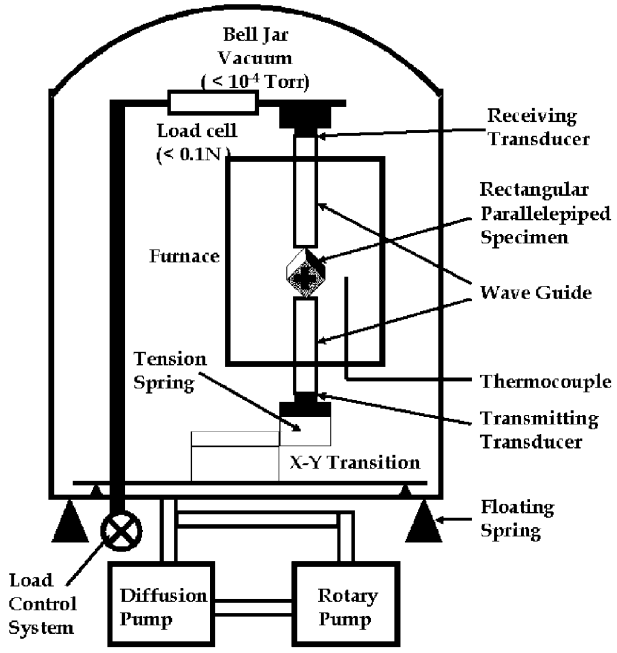

Fig. 2. A high temperature device for RUS experiment.

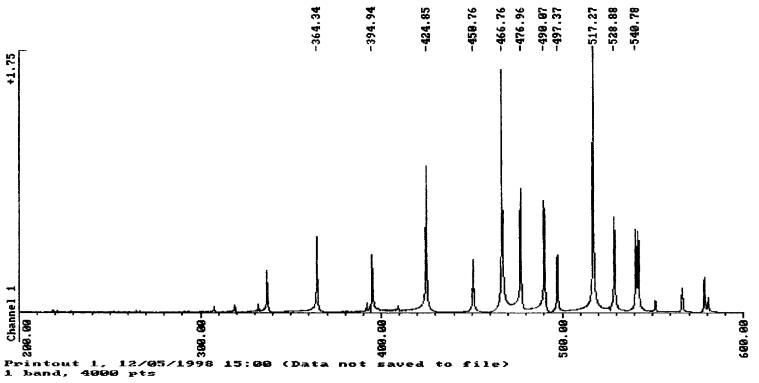

Fig. 3. Typical resonance spectrum of rectangular parallelepiped Zr–2.5Nb pressure tube material. Vertical axis is the intensity and horizontal axis is the frequency in kHz.

uum environment the distance between the thermocouple and specimen was kept <5 mm and maintained more than 1 h before the measurement. Temperature difference by a dummy thermocouple on the specimen was less than ±2 °C in the experimental temperature range. There was no difference in the resonance frequencies and subsequent elastic constants between the conditions of vacuum environment and normal atmosphere.

Rectangular parallelepiped Zr–2.5Nb samples were machined accurately, with dimensions of 2.5 mm × 3.0 mm × 3.5 mm. Calculated frequencies by an input of dimensions, density, symmetry and initial estimate of elastic stiffness corresponded to the measured frequencies and vibration modes. Fig. 3 shows a typical resonance ultrasound spectrum of the Zr–2.5Nb alloy. The initial 30 resonant frequencies were calculated and compared with measured values. Table 3 shows a typical example of calculated anisotropic elastic stiffness of Zr–2.5Nb pressure tube at room temperature by RUS, with abbreviations of k, l, $f_{\text{calc.}}$ and $f_{\text{meas.}}$ denoting the resonance mode, number of harmonics, calculated resonance frequency by initial estimate of elastic stiffness, and measured resonance frequency by RUS, respectively. The initial 30 resonance frequencies are located in the range of 200–600 kHz. After iteration and convergence, the final RMS errors were in the range of 0.05–0.1%, which can be compared with the RMS error of <0.2%, and can be regarded as reliable and accurate.

5. Results and discussion

5.1. Anisotropic elastic stiffness by RUS and ODF model at room temperature

Table 4 shows the anisotropic elastic stiffness of the Zr–2.5Nb alloy by RUS. Table 5 shows Young's moduli, which are the inverse of the elastic compliance, $E_{ii} = 1/S_{ii}$. Based on the pole figures for (0 0 0 2) in Fig. 1, f-coefficients or Kearn's factors, which represent the degree of orientations along the c-axis, are calculated as $f_{\text{T}} = 0.6$, $f_{\text{R}} = 0.33$ and $f_{\text{L}} = 0.07$, where the subscripts denote T: transverse, R: radial and L: longitudinal direction [17,18]. This fact implies that ≈60% of the (0 0 0 2) pole is aligned along the transverse direction (or circumferential direction), 33% along the radial direction, and 7% along the longitudinal direction. Because the elastic stiffness along the c-axis in the single crystal zirconium is greater than along the a-axis, i.e. $c_{33} > c_{11}(= c_{22})$ (subscripts follow single crystal coordinate; $1(= 2) = a$-axis, $3 = c$-axis in hcp crystalline structure), the elastic stiffness along a direction of a higher f-coefficient should be greater than along the other directions. In addition, the elastic stiffness estimated by ODF or RUS results in $c_{\text{TT}} > c_{\text{RR}} > c_{\text{LL}}$ (subscripts follow sample coordinate; R: radial direction, T: transverse direction, L: longitudinal direction), which indicates the highest elastic stiffness is along the transverse direction and the lowest along the longitudinal direction, which is in accordance with the expectation.

There are small differences between the elastic stiffness by ODF and by RUS, as shown in Tables 2 and 4. The elastic stiffness estimated by ODF is based on the orientation distribution of an individual crystallite. All models for macroscopic (specimen) properties from microscopic (crystallite) properties, such as Voight's approximation or the Reuss approximation, share common assumptions: (i) absence of voids, non-homogeneity, (ii) cohesion of crystallites occur through very thin grain boundary regions that are deformed relative to the crystal interiors, (iii) randomly orientated grains and (iv) grains large enough so that interfaces remain non-important [7]. In addition, microscopic variations, such as size and shape of crystallites, the effect of alloying elements, the existence of a β-phase, dislocation density

Table 3
An example of calculation for anisotropic elastic stiffness of Zr–2.5Nb pressure tube by RUS

n	k	l	$f_{calc.}$ (MHz)	$f_{meas.}$ (MHz)	ZR4B025 error (%)	Percentage of modulus contributing to mode								
						c_{11}	c_{22}	c_{33}	c_{23}	c_{13}	c_{12}	c_{44}	c_{55}	c_{66}
1	4	1	0.22592	0	0	0.01	0.01	0.01	0	−0.01	−0.01	0.64	0.3	0.05
2	4	2	0.30677	0.30722	−0.15	0.01	0.02	0.04	−0.02	−0.01	0	0.05	0.36	0.55
3	1	1	0.31874	0.31899	−0.08	0.06	0.34	1.06	−0.58	−0.26	0.13	0	0.22	0.02
4	7	1	0.33195	0.33206	−0.03	0.33	0.05	1.08	−0.22	−0.61	0.12	0.24	0	0.01
5	8	2	0.33503	0.33528	−0.07	0.03	0.02	0.05	0	−0.03	−0.01	0.95	0	0
6	2	1	0.36381	0.36401	−0.06	0.02	0.04	0.08	−0.05	−0.01	−0.01	0	0.92	0
7	5	1	0.39311	0.39258	0.13	0.24	0.37	1.41	−0.69	−0.58	0.27	0	0	0
8	6	1	0.39414	0.39407	0.02	0.47	0.95	0.03	−0.11	0.07	−0.67	0.22	0.03	0
9	3	2	0.39424	0.39438	−0.04	0.05	0.08	0.2	−0.11	−0.09	0.03	0.01	0	0.82
10	1	2	0.40886	0.40867	0.05	0.22	0.74	0.07	0.01	−0.05	−0.38	0.01	0.1	0.27
11	3	3	0.42385	0.4239	−0.01	0.07	0.06	0.6	−0.17	−0.2	0.05	0.08	0.09	0.43
12	5	2	0.42416	0.42437	−0.05	0.66	0.68	0.66	−0.25	−0.38	−0.38	0	0	0
13	2	2	0.45094	0.45124	−0.07	0.09	0.89	0.12	−0.32	0.09	−0.27	0.03	0.24	0.12
14	5	3	0.45227	0.45234	−0.02	0.99	1.02	0.01	0.08	−0.09	−1	0	0	0
15	3	4	0.46623	0.4662	0.01	0.08	0.05	0.19	−0.04	−0.1	−0.02	0.35	0.38	0.09
16	7	2	0.47757	0.47711	0.1	0.82	0.16	0.08	0.05	−0.19	−0.33	0.2	0.01	0.2
17	6	2	0.48984	0.48971	0.03	0.67	0.07	0.25	−0.04	−0.38	0	0.19	0.23	0.01
18	8	3	0.49608	0.49645	−0.07	1.14	0.11	0.21	0.14	−0.51	−0.34	0.19	0.01	0.05
19	4	3	0.51632	0.51577	0.11	0.02	0.03	0.04	0	−0.01	−0.01	0.25	0.29	0.4
20	2	3	0.52516	0.52475	0.08	0.11	0.2	0.11	−0.05	−0.06	−0.1	0.39	0.09	0.3
21	5	4	0.52866	0.52928	−0.12	0.58	0.21	0.82	−0.29	−0.54	0.14	0.03	0.04	0.02
22	6	3	0.53954	0	0	0.53	0.62	0.51	−0.31	−0.29	−0.22	0.1	0.07	0
23	1	3	0.54105	0	0	0.21	0.64	0.49	−0.29	−0.14	−0.21	0	0.2	0.09
24	7	3	0.54106	0.5414	−0.06	0.57	0.34	0.53	−0.21	−0.25	−0.25	0.19	0.01	0.06
25	5	5	0.55249	0.55226	0.04	0.81	0.79	0.1	−0.06	−0.05	−0.63	0.02	0.01	0.01
26	8	4	0.56607	0.56557	0.09	0.29	0.2	0.25	−0.09	−0.15	−0.13	0.08	0.32	0.23
27	7	4	0.56638	0.56603	0.06	0.36	0.14	0.43	−0.18	−0.22	−0.02	0.38	0	0.1
28	1	4	0.57873	0.57809	0.11	0.16	0.07	0.45	−0.13	−0.26	0.07	0	0.56	0.08
29	6	4	0.58083	0	0	0.45	0.55	0.12	−0.15	0.01	−0.37	0.27	0.11	0
30	6	5	0.60254	0.60246	0.01	0.64	0.12	0.85	−0.21	−0.75	0.15	0.03	0.16	0
Elastic moduli (dynes × 10^{12}/cm^2)						1.4737	1.5449	1.4717	0.7429	0.7693	0.7612	0.3338	0.3397	0.3672

Dimensions (cm)	Initial	Adjusted
d1	0.35300	0.35023
d2	0.40100	0.40259
d3	0.4490	0.45077
RMS error	0.074200	

Table 4
Anisotropic elastic stiffness of Zr–2.5Nb pressure tube by RUS (unit: 10^{11} N/m^2)

c_{11}	c_{22}	c_{33}	c_{23}	c_{13}	c_{12}	c_{44}	c_{55}	c_{66}
1.4708	1.5269	1.4533	0.7191	0.7538	0.7446	0.3381	0.3425	0.3696

Notation of sample orientation: 1 = RD (radial direction), 2 = TD (transverse direction), 3 = LD (longitudinal direction).

and distribution, are not reflected in the estimation by ODF. On the contrary, RUS can give us realistic elastic stiffness value without any assumption.

One of the important factors in determining elastic stiffness by RUS is that the initial input of the elastic stiffness be close enough to the true values in order to converge during the iteration processes. In an earlier study, we attempted the averaging method by *f*-coefficients from X-ray pole figure data. Using those values as the initial input for RUS calculations, relatively high

Table 5
Anisotropic elastic moduli of Zr–2.5Nb pressure tube converted from the elastic compliance (unit: 10^9 N/m^2)

Young's moduli			Shear moduli			Bulk modulus
E_{11}	E_{22}	E_{33}	G_{44}	G_{55}	G_{66}	K
96.18	104.32	96.79	33.81	34.59	36.96	98.70

Notation of sample orientation: 1 = RD (radial direction), 2 = TD (transverse direction), 3 = LD (longitudinal direction).

RMS errors between calculated and measured frequencies indicated the RUS measurement was not reliable. It seems that *f*-coefficients, which imply simple fractions of crystallites along the three major axes, could not be a proper approximation to obtain a nine independent elastic stiffness for the specimen. However, using the initial estimates by the self-iteration method based on the ODF model and elastic constant of zirconium single crystal, RMS error in the range of 0.05–0.1% indicates the results are very accurate. Generally RMS error $<$ 0.2% is required for the reliable RUS experiment [14]. An example of RUS results is shown in Table 3.

It is not easy to obtain an elastic modulus along the radial or transverse direction in the tubular shaped sample by conventional methods. It has been reported that the approximated elastic modulus for α-zirconium is 98.6 GPa [19]. Ashida et al. [20] reported a relation of the Young's modulus to temperature as $E = -0.0656T + 115.1$ by measurement of resonance frequencies in the bending and torsion test, which comes out the Young's modulus of 95.4 GPa at room temperature. Northwood et al. [21] reported that Young's moduli of Zr–2.5Nb alloy are $E_L = 97.0$ GPa, $E_T = 95.2$ GPa, $G = 35.9$ GPa. All these reported values are restricted to a certain direction or assumption of isotropic properties. However, as shown in Table 5, RUS can determine all the elements of elastic stiffness, including Young's moduli along the radial, transverse, and longitudinal directions as well as the shear moduli and bulk modulus at once. Because of the differences in materials, especially in anisotropic properties, small differences of the elastic moduli are quite natural.

5.2. Temperature dependence of anisotropic elastic constants of Zr–2.5Nb pressure tube

Fig. 4 shows the c_{ij} of Zr–2.5Nb pressure tube materials in the range of room temperature ~500 °C, with the subscripts 'l', 't', 'r' denoting longitudinal, transverse and radial direction, respectively. Fig. 5 shows the Young's moduli and shear moduli.

The elastic constants decrease as the temperature increases and the elastic constants along the transverse direction are clearly higher than those along the radial or longitudinal direction. As shown in Fig. 4, the elastic stiffness values are positioned within the c_{33} and c_{11} of single crystal zirconium, which is the upper and lower

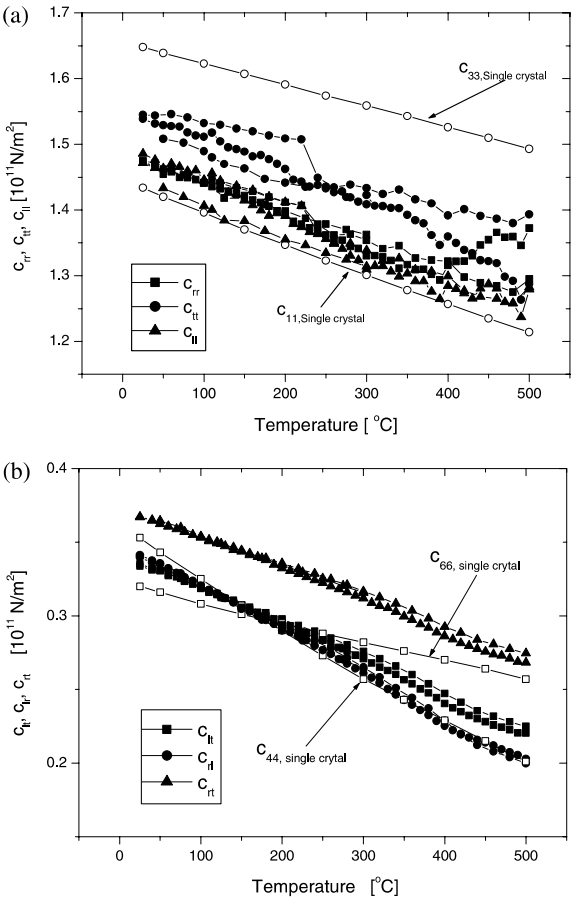

Fig. 4. Temperature dependency of elastic stiffness of Zr–2.5Nb pressure tube material. (a) Normal components of elastic stiffness. (b) Shear components of elastic stiffness.

bound [16]. Because (0 0 0 2) pole is not a major orientation along the radial or longitudinal direction, more random orientation distribution is expected and there is little difference in the elastic constant along the radial direction and those along the longitudinal direction. Young's modulus and shear modulus show a similar tendency in Fig. 5.

A crossing phenomenon of the shear component of elastic stiffness along the longitudinal direction and radial direction are observed in the temperature range of 120–150 °C. There are several possibilities to explain the

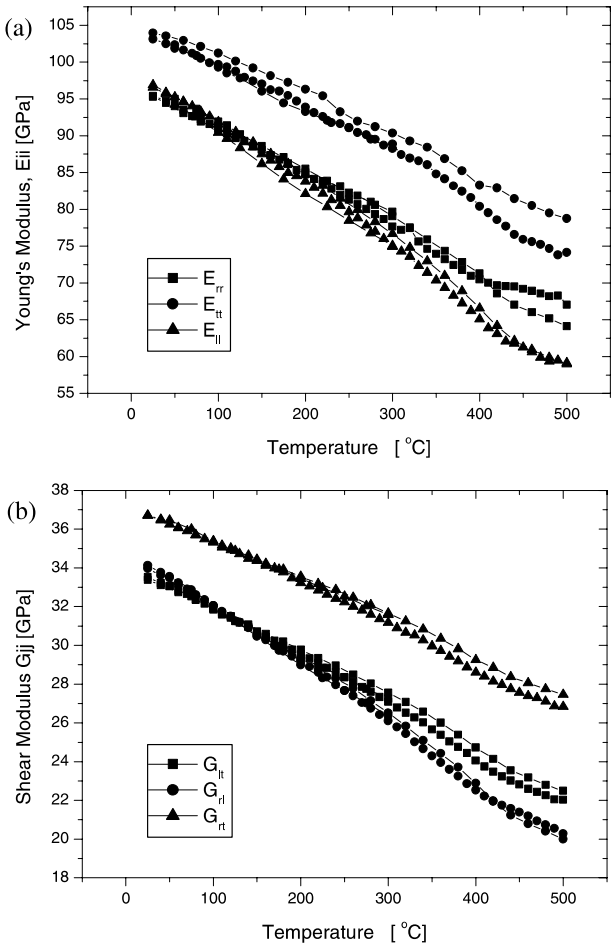

Fig. 5. Temperature dependency of elastic moduli of Zr–2.5Nb pressure tube material. (a) Young's moduli of pressure tube. (b) Shear moduli of pressure tube.

phenomenon: (1) relaxation of the hydrogen atom in the zirconium lattice (Bordoni peak) [22]; (2) intrinsic characteristics of the crossing of c_{44} and c_{66} of a zirconium single crystal; (3) transition of the α-Zr + hydrogen atom and metastable γ-hydride (or stable δ-hydride); and (4) phase transition of γ-hydride to δ-hydride [23]. As shown in Fig. 4, this fact could correlate to the crossing characteristics of c_{44} and c_{66} of a zirconium single crystal in the temperature range. However, the reason why the crossing characteristics occurred in the temperature range is not clear at this point. Since the mechanical damping, Q^{-1} or high frequency ultrasonic loss is related to the microstructural inhomogeneities and calculated from the width of resonance peak, further investigation of the resonance frequencies as well as a mechanical damping, Q^{-1} on the zirconium material with various hydrogen contents might be useful to explain the crossing phenomenon. Mechanical damping, Q^{-1} could be correlated to the content and status of hydrogen atom in zirconium lattice.

6. Conclusion

1. The dynamic anisotropic elastic stiffness of Zr–2.5Nb pressure tube materials has been determined by RUS. The initial estimate for RUS has been obtained from a consideration of ODF by X-ray pole figures and the elastic stiffness of a single crystal zirconium.
2. There is a small difference between the elastic stiffness by ODF model and RUS at room temperature. It implies that the values by RUS are closer to the true values.
3. The elastic constant c_{ij} decreases gradually as the temperature increases. The elastic constants along the transverse direction are greater than those along

the longitudinal or radial direction. This tendency agreed with the case of Young's moduli or shear moduli.

4. The longitudinal component and radial component of shear moduli are crossed at 120–150 °C. This fact could correlate to the crossing characteristics of the c_{44} and c_{66} of a zirconium single crystal in the temperature range.
5. RMS error of $<0.2\%$ by RUS indicates the measurements are reliable and accurate.
6. The RUS method is a very sensitive tool for determining the elastic constants. It can be a useful method for characterizing the effect of material degradation due to neutron irradiation.

Acknowledgements

This work was supported by the CANDU pressure tube materials project, as a part of the long-term nuclear research program by the Ministry of Science and Technology. The authors would like to express their appreciation to Dr Yong-Che Kim for sincere discussions on the theory of ODF and analysis of X-ray pole figures.

References

[1] L.D. Landau, E.M. Lifshitz, in: Theory of Elasticity, 2nd Ed., Pergamon, London, 1970, p. 37.
[2] Y.C. Kim, H.J. Kim, B.C. Chun, C.H. Lee, J.S. Lee, B.S. Seong, H.S. shim, B.H. Choi, J.W. Ho, J. Kor. Inst. Met. Mater. 29 (1991) 866.
[3] M.L. Dunn, H. Ledbetter, P.R. Heyliger, C.S. Choi, J. Mech. Phys Solids 44 (1996) 1509.
[4] R.J. Roe, J. Appl. Phys. 36 (1965) 2024.
[5] H.J. Bunge, in: Texture Analysis on Materials Science, Butterworth, London, 1982, p. 97 (Translated by P.R. Morris).
[6] P.R. Morris, J. Appl. Phys. 40 (1969) 447.
[7] H. Ledbetter, in: A. Wolfenden (Ed.), Dynamic Elastic Modulus Measurements in Materials, ASTM STP 1045, American Society for Testing and Materials, Philadelphia, PA, 1990, p. 135.
[8] A. Miglioli, W.M. Visscher, S.E. Brown, Z. Fisk, S.W. Cheong, B. Alten, E.T. Ahrens, K.A. Kubat-Martin, J.D. Maynard, Y. Huang, D.R. Kirk, K.A. Gillis, H.K. Kim, M.H.W. Chan, Phys. Rev. 41 (1990) 2098.
[9] J.D. Maynard, J. Acoust. Soc. Am. 91 (1992) 1754.
[10] R. Holland, J. Acoust. Soc. Am. 43 (1968) 988.
[11] H.H. Demarest, J. Acoust. Soc. Am. 49 (1971) 768.
[12] I. Ohno, J. Phys. Earth 24 (1976) 355.
[13] A. Migliori, J.L. Sarrao, W.M. Visscher, T.M. Bell, M. Lei, Z. Fisk, R.G. Leisure, Physica B 183 (1993) 1.
[14] A. Migliori, J. Sarrao, in: Resonant Ultrasound Spectroscopy, Wiley, New York, 1997, p. 53.
[15] S.I. Wright, U.F. Kocks, PopLA, Preferred Orientation Package – Los Alamos, Los Alamos National Laboratory, 1995.
[16] E.S. Fisher, C.J. Renken, Phys. Rev. 135 (2A) (1964) A482.
[17] Y.S. Kim, K.N. Choo, C.H. Chung, K.S. Lim, S.S. Kim, J.H. Paek, Y.H. Chung, K.H. Kim, Development of Zirconium Alloys for Pressure Tubes, Final Report, KAERI/RR-1766-96, Korea Atomic Energy Research Institute, South Korea, 1997.
[18] K.S. Choo, S.C. Kwon, Y.S. Kim, J. Kor. Nucl. Soc. 30 (4) (1998) 318.
[19] P.K. De, J.T. John, S. Banerjee, T. Jayakumar, M. Thavasimuthu, B. Raj, J. Nucl. Mater. 252 (1998) 43.
[20] Y. Ashida, M. Yamamoto, S. Naito, M. Mabuchi, T. Hashino, J. Appl. Phys. 80 (1996) 3254.
[21] D.O. Northwood, I.M. London, L.E. Bahen, J. Nucl. Mater. 55 (1975) 299.
[22] V. Provenzano, P. Schiller, A. Schneiders, J. Nucl. Mater. 52 (1974) 75.
[23] J.H. Root, W.L. Fong, J. Nucl. Mater. 232 (1996) 75.